

See discussions, stats, and author profiles for this publication at: <https://www.researchgate.net/publication/273128087>

# A Hybrid Statistical Mechanics—Quantum Chemical Model for Proton Transfer in 5-Azauracil and 6-Azauracil in Water Solution

ARTICLE in INTERNATIONAL JOURNAL OF QUANTUM CHEMISTRY · APRIL 2015

Impact Factor: 1.43

---

READS

49

## 3 AUTHORS:



Venelin Enchev

Bulgarian Academy of Sciences

103 PUBLICATIONS 807 CITATIONS

SEE PROFILE



Ljupco Pejov

Ss. Cyril and Methodius University

108 PUBLICATIONS 846 CITATIONS

SEE PROFILE



Nadezhda Markova

Bulgarian Academy of Sciences

20 PUBLICATIONS 184 CITATIONS

SEE PROFILE

# A Hybrid Statistical Mechanics—Quantum Chemical Model for Proton Transfer in 5-Azauracil and 6-Azauracil in Water Solution

Nadezhda Markova,<sup>[a]</sup> Ljupco Pejov,<sup>[b,c]</sup> and Venelin Enchev<sup>\*,[a]</sup>

A hybrid statistical physics—quantum-chemical methodology was implemented to study the water-assisted intramolecular proton-transfer processes in 5- and 6-azauracils in aqueous solutions. The solvent effects were included in the model by explicit inclusion of two pairs of water molecules, which model the relevant part of the first hydration shell around the solute. The position of these water molecules was initially estimated by carrying out a classical Metropolis of dilute water solutions of the title compounds and subsequently analyzing solute–solvent intermolecular interactions in the Monte Carlo-generated configurations. Sequentially to the statistical physics simulation, *ab initio* quantum mechanical (QM) level of theory was implemented. The effects of the water as solvent (at *ab initio* QM level) were introduced at two different levels—using solute–solvent clusters (four-water molecules) and using the same clusters embedded in an external continuum. Full geometry optimizations of these complexes were carried out at MP2/6–31 + G(d, p) and conductor-polarizable continuum model (C-PCM)/MP2/6–31 + G(d, p). Single point calculations

were performed at CCSD(T)/6–31 + G(d, p)//MP2/6–31 + G(d, p) computational level to obtain more accurate energies. According to our calculations hydrated azauracils should exist in three forms: mainly dioxo form and two hydroxy forms. The calculated proton transfer activation energies for tautomeric reactions of 5-azauracil and 6-azauracil show different pictures for these two compounds. According to C-PCM/MP2/6–31 + G(d, p) data, water-assisted proton transfer in 5-azauracil realizes through two parallel reactions: 1,3,5-triazine-2,4(1H,3H)-dione → 6-hydroxy-1,3,5-triazin-2(1H)-one and 1,3,5-triazine-2,4(1H,3H)-dione → 4-hydroxy-1,3,5-triazin-2(1H)-one. Tautomeric equilibrium in 6-azauracil in water could occur by two contiguous reactions: 1,2,4-triazine-3,5(2H,4H)-dione → 5-hydroxy-1,2,4-triazin-3(2H)-one and 5-hydroxy-1,2,4-triazin-3(2H)-one → 3-hydroxy-1,2,4-triazin-5(2H)-one. The proton transfer investigated reactions in 5- and 6-azauracils involve concerted atomic movement. © 2015 Wiley Periodicals, Inc.

DOI: 10.1002/qua.24871

## Introduction

Tautomerism plays a key role in biological systems,<sup>[1]</sup> from DNA base-pairing<sup>[2–6]</sup> to the regulation of the function and activity of various enzymes.<sup>[7,8]</sup> Many of these biological effects rely not only on the presence of different tautomers but also on the rate at which they interconvert. Hydration plays a significant role in the tautomeric process. A water molecule may influence the stability of different tautomeric forms through hydrogen-bonding interactions. Conversely, the water-assisted proton transfer has been shown to increase the populations of the minor tautomers greatly by lowering the activation energy barrier of the proton transfer reaction.<sup>[9–21]</sup> Affecting the structures and the properties of solute, the binding solvent molecules may profoundly influence reactivity by altering the environment around the solute or they may directly participate in the dynamic processes as in solvent-mediated chemical reactions. In the literature, water has been shown to be important as a catalyst mediating proton transfer.<sup>[22,23]</sup>

Aza analogues of nucleobases are of special interest due to their biological and pharmacological activities. Among possible structural modifications of uracil, one may consider the ring alternations via the substitution of the CH groups by nitrogen atom. In this way, one may obtain the 5- and 6-azauracils (Fig. 1). The biological activities of aza analogues of uracil have

been intensively investigated. The 5- and 6-azauracils have been described to possess anticancer, antidepressant, hypnotic, antiallergic, antiasthmatic, anxiolytic, antidepressant, and anticonvulsant properties.<sup>[24]</sup>

5-azauracil (1,3,5-triazine-2,4(1H,3H)-dione, 5-AU) is considered to be a potential anticancer agent. Experimental investigations<sup>[25–28]</sup> performed in gas phase, solid state, or in solution indicate that the amino-oxo tautomer of 5-azauracil is the most stable one. Infrared spectra of 5-azauracil in dioxan and ethanol solutions indicate the presence of the dioxo tautomeric form.<sup>[25]</sup> Interpretation of the UV spectra of 5-azauracil in water is ambiguous.<sup>[25]</sup> The tautomerism of 5-azauracil in

[a] N. Markova and V. Enchev  
Institute of Organic Chemistry, Bulgarian Academy of Sciences, 1113 Sofia, Bulgaria  
E-mail: venelin@orgchem.bas.bg

[b] L. Pejov  
Faculty of Natural Sciences and Mathematics, Institute of Chemistry, Arhimedova 5, Skopje, Macedonia

[c] L. Pejov  
Research Centre for Environment and Materials, Macedonian Academy of Sciences and Arts, Krste Misirkov 2, 1000, Skopje, Macedonia

Contract grant sponsor: DNTS/Macedonia 01–14/2011, Project BAS–MANU, Bulgarian Ministry for Education and Science [Project BG051PO001/3.3–05–0001]; contract grant number: DO3–151.

© 2015 Wiley Periodicals, Inc.

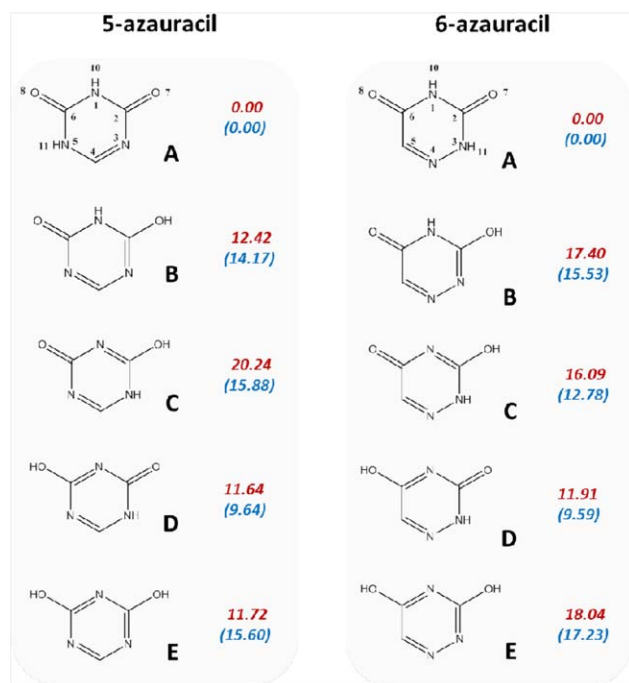


**Figure 1.** Possible tautomeric forms of 5-azauracil and 6-azauracil, and their calculated MP2/6-31 + G(d, p) relative energies ( $\Delta G_{298}$ ) in kcal mol<sup>-1</sup> in gas phase and in solution (in brackets).

deuterated dimethyl sulfoxide (DMSO) was investigated by Pike<sup>[26]</sup> by means of Nuclear Magnetic Resonance (NMR) spectroscopy, but his results were not conclusive.

6-azauracil (1,2,4-triazine-3,5(2H,4H)-dione, 6-AU) was formerly used as an antitumor drug and has been studied extensively. Many experimental and theoretical studies have revealed its structural, chemical, and spectroscopic properties.<sup>[28–42]</sup> The crystal structure of 6-azauracil is reported by Singh and Hodgson.<sup>[29,39]</sup> 6-azauracil was the subject of quantum chemical studies.<sup>[40–42]</sup> In *ab initio* quantum chemical study, Les and Ortega-Blake<sup>[42]</sup> concluded that the 3-NH tautomer has been preferred over the 4-OH tautomer in the gas phase by 10.2 kcal/mol.

Recently, investigations on the tautomerism of 5-azauracil and 6-azauracil anions<sup>[43,44]</sup> were published. However, there are not studies on tautomeric conversions in solution (particularly, water) of neutral azauracils. While the structures of azapyrimidines would be expected to be quite similar to those of the corresponding pyrimidines, the concept of their tautomerism is important to the structure of nucleic acids. As there are findings that 6-azauracil derivatives of 4,5 didehydro-5,6-dideoxy-L-ascorbic acid possess pronounced cytostatic activity against some malignant tumour cell lines, the idea of tautomeric conversion in such compounds attains significant importance.<sup>[45]</sup>

At this point of view, the subject of this study is the tautomerization of 5- and 6-azauracils in the presence of binding water molecules. We report the dynamic pathways between the dioxo and hydroxy tautomeric forms of these compounds.

We consider the effect of hydration using the supermolecule approach in which four-water molecules forming two clusters are attached to the azauracil tautomers. To avoid the inherent

arbitrariness, or the necessity of relying on “classical chemical intuition” in the way in which the solvent influence on the tautomerism is accounted for, we implement a two-phase hybrid statistical physics—quantum-chemical approach to this phenomenon. The two-phase approach is based on sequential Metropolis Monte Carlo (MC) simulation followed by analysis of solute–solvent interaction network patterns and subsequent finite cluster quantum mechanical (QM) study of the proton-transfer process influenced by water as solvent. The hydration by bulk water is covered by the self-consistent reaction field (SCRF) method using the conductor-polarizable continuum model (C-PCM) approach.<sup>[46]</sup>

## Computational Details

The common practice for optimizing a molecule in solution is the application of some continuum dielectric method<sup>[46–58]</sup> where the solute is placed in a cavity carved into the solvent. Such a cavity may be constructed to a different level of sophistication, starting from a simple spherical cavity with radius computed from the molecular van der Waals volume, up to the cavities closely matching the solute molecular shape. The solvent is modeled generally as a polarizable dielectric continuum characterized by its bulk dielectric constant and some other parameters accounting for nonelectrostatic solute–solvent interaction terms. The advantage of this approach is that it accounts for the very important long-range electrostatic interactions in a fairly simple way. However, the major weakness of the continuum solvent approach is that a structureless medium does not take into consideration the QM consequences of hydrogen-bond interactions between solute and solvent or any other specific noncovalent solvent–solute intermolecular interaction.

In addition in protic solution, a solvent-catalyzed mechanism of tautomeric reactions is also possible. Thus, the solvent does not simply exert a through-space effect, but it rather becomes an active participant in the process. The hydrogen-bonded proton of the solute is picked up by a protic solvent molecule and is returned into a new position of the solute by another solvent molecule. This mechanism hypothesizes the existence of a solvent network around the solute, which is certainly true in aqueous solution. If one wants to explore the most favorable arrangements of the water molecules around the solute, preliminary model calculations are useful for optimizing the positions of a limited number of the water molecules. Calculations in the gas phase provide the optimized structure of gas-phase hydrates, and will be called supermolecule approach. If the hydrate structure is reoptimized by means of a continuum dielectric solvent method when the hydrate is placed into a cavity carved within the polar solvent, the approach is called the supermolecule + continuum. This approach allows for charge transfer between the central solute and the explicit solvent molecules, which affect the derived atomic charges for the solute while the long-range solvent influence is also accounted for.

In this study, we model the water-assisted proton transfer in 5- and 6-azauracil. The most rigorous approach that we implement for that purpose is the supermolecule + continuum

approach. To complement, however, the supermolecular methodology and to further justify the particular bonding pattern used to derive conclusions about the water-assisted proton transfer in solution as well as to judge on the relative hydration energies of various tautomeric forms, we have also carried out rigid-body MC simulations of various forms of 5-azauracil and 6-azauracil in diluted aqueous solutions.

### Monte Carlo simulations

MC simulations of 5-azauracil and 6-azauracil water solutions carried out for the purpose of the present study were of a rigid-body type, that is, the intramolecular parameters of both the solute and solvent molecules were kept fixed throughout the simulation. The geometries of 5-azauracil and 6-azauracil used for the rigid-body MC simulations were those corresponding to the minima on the MP2/6-31 + G(d, p) potential energy hypersurfaces (PESs), as located by the GAMESS program package.

Series of MC simulations in the isothermal-isobaric (NPT) ensemble were carried out to generate the structure of the studied liquids. The statistical mechanics code DICE was used for these purposes.<sup>[59]</sup> The Metropolis sampling algorithm was implemented for all MC simulations, which were actually carried out at  $T = 298$  K,  $P = 1$  atm. In each MC simulation, a single 5- or 6-azauracil tautomer was surrounded by 500 water molecules in a cubic box with side length of approximately 25 Å (using the experimental density of liquid water of 0.9966 g cm<sup>-3</sup> at these conditions). Periodic boundary conditions were imposed, and the long-range corrections to the interaction energy were calculated for interacting atomic pairs between which the distance is larger than the cut-off radius defined as half of the unit cell length. The Lennard-Jones contribution to the interaction energy beyond this distance was estimated assuming uniform density distribution in the liquid (i.e.,  $g(r) \approx 1$ ). The electrostatic contribution was, conversely, estimated by the reaction field method involving the dipolar interactions. In all MC simulations carried out in this study, intermolecular interactions were described by a sum of Lennard-Jones 12-6 site-site interaction energies plus Coulomb terms:

$$U_{ab} = \sum_i^a \sum_j^b 4\epsilon_{ij} \left[ \left( \frac{\sigma_{ij}}{r_{ij}} \right)^{12} - \left( \frac{\sigma_{ij}}{r_{ij}} \right)^6 \right] + \frac{q_i q_j}{4\pi\epsilon_0 r_{ij}} \quad (1)$$

where  $i$  and  $j$  are sites in interacting molecular systems  $a$  and  $b$ ,  $r_{ij}$  is the interatomic distance between sites  $i$  and  $j$ , and  $e$  is the elementary charge. The following combination rules were used to generate two-site Lennard-Jones parameters  $\epsilon_{ij}$  and  $\sigma_{ij}$  from the single-site ones:

$$\epsilon_{ij} = \sqrt{\epsilon_i \epsilon_j} \quad (2)$$

$$\sigma_{ij} = \sqrt{\sigma_i \sigma_j} \quad (3)$$

For water, we have used the simple point-charge (SPC) model potential parameters<sup>[60]</sup> while the charge distribution in the case of various tautomeric forms of 5- and 6-azauracils were calculated by fitting the individual (atomic) charges, cen-

tered at atomic positions, to the molecular electrostatic potential computed from the QM wavefunction (MP2/6-31 + G(d, p)) at series of points selected by the CHarges from Electrostatic Potentials using a Grid based method (CHELPG) algorithm<sup>[61]</sup> with an additional constraint that the molecular dipole moment is correctly reproduced by the chosen set of point charges. In the fitting procedure, the MP2 electronic density was used as a reference in all cases. The Lennard-Jones parameters for azauracils were taken from the Optimized Potentials for Liquid Simulations (OPLS) force field database.<sup>[62]</sup> All simulations consisted of thermalization phase of at least  $5.0 \times 10^7$  MC steps, which was subsequently followed by averaging (simulation) phase of at least  $4.5 \times 10^8$  MC steps.

### Ab initio calculations

*Ab initio* quantum chemical calculations were performed for 5- and 6-azauracils in gas phase, in a four-water cluster and the same clusters embedded in an external continuum. The geometries of the possible tautomeric forms, their four-water complexes and the respective transition states (TSs) with and without external continuum, were located at MP2/6-31 + G(d, p) level of theory. The C-PCM formalism<sup>[46]</sup> at MP2 level was applied to account structure-less dielectric medium. The calculations were done without symmetry constraints by the gradient procedure. A gradient convergence threshold of  $1 \times 10^{-5}$  hartree Bohr<sup>-1</sup> was used. All the minima and TSs were confirmed by normal mode analysis at the same computational level as used for the geometry optimization. The Hessians of the local minima had zero and those of the TSs only one negative eigenvalues, respectively. Starting from the TS, the reaction path was generated as the steepest descent path in mass-scaled coordinates (intrinsic reaction coordinate) using the Gonzalez-Schlegel algorithm,<sup>[63]</sup> using a step size of 0.05 Bohr (1 Bohr corresponds to 0.53 Å). On both branches of the reaction coordinate 40 steps were performed. The values of Gibbs free energies ( $\Delta G$ ) and activation barriers ( $\Delta G^\ddagger$ ) were calculated at a temperature of 298.15 K. The classical rate constant at 298.15 K was calculated using the Eyring equation,  $k = (k_B T/h) \cdot e^{-\Delta G/RT}$ , where  $k_B$  and  $h$  are the Boltzmann and Planck constants, respectively. The values of the populations ( $p_i$ ) were calculated by the standard formula  $p_i = e^{-\Delta G_i/RT} / \sum e^{-\Delta G_i/RT}$ .

Single-point calculations were further performed at the coupled cluster (CCSD(T)) level<sup>[64–68]</sup> with the same basis set to refine the relative energies of the stationary points.

All calculations were carried out using the GAMESS (US) quantum chemistry package.<sup>[69]</sup>

## Results and Discussion

The five possible tautomeric forms of 5-AU and 6-AU are shown in Figure 1. All species were optimized at MP2/6-31 + G(d, p) level of theory. The relative Gibbs free energies of the dioxo **A** and different hydroxy tautomers **B–E** of the azauracils in gas phase are also presented in Figure 1. The computed energies of the tautomers studied reveal that at MP2/6-

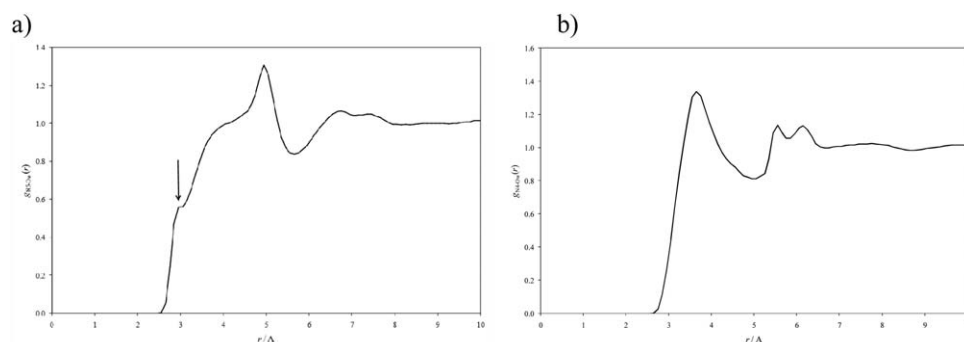


**Figure 2.** The RDF between: a) N5 center of 5-azauracil and water oxygen and b) N4 center of 6-azauracil and water oxygen, computed from the equilibrated MC run.

31 + G(d, p) level of theory the dioxo form **A** of 5-AU is the most stable one, followed by the hydroxy forms **D**, **E**, **B**, and **C**. The stability sequence of 6-AU is **A** > **D** > **C** > **B** > **E**. The relative stabilities of isolated tautomeric forms of the azauracils are considered only for comparison because of stability sequence alteration on hydration. When all species of 5-AU and 6-AU were optimized again using C-PCM at MP2/6-31 + G(d, p) level in water as medium, the energy sequences are not changed for 6-AU. There is change in the relative stability order of the tautomers of 5-AU—in water tautomer **B** became more stable than **E** (Fig. 1).

#### Differential hydration and hydrogen bonding in diluted aqueous solutions

We further analyze in details the hydrogen bonding between various tautomeric forms of 5-AU and 6-AU (Fig. 1) and solvent water molecules. Both the proton-donating and the proton-accepting abilities of the solvent and solute molecules are considered. However, to count the number of hydrogen-bonding interactions in which each center within the solute molecule takes part is far from a trivial task. To avoid any arbitrariness, and also to correctly account for all fundamental criteria for this noncovalent interaction in solution, we adopt the following multistep procedure, which we illustrate through the particular example of the H-bonding acceptor properties of the N5 center within the tautomer **A** of 5-AU. For comparison purposes, the analogous parameters have only briefly been illustrated in the case of 6-AU as well. One parameter which certainly is of importance for establishing whether a hydrogen-bonding interaction (X—H...Y) between a given proton donor (X—H) and proton acceptor (Y) occurs is the X...Y distance. The radial distribution function (RDF) between the N5 center within tautomer **A** of 5-azauracil and the O atom of the solvent water molecules ( $O_w$ ) is shown in Figure 2a. Figure 2b shows the corresponding N4... $O_w$  RDF in the case of 6-AU.

The first peak seen in this RDF (marked by an arrow in Fig. 2a) implies an existence of certain population of first-shell water molecules positioned close to the N5 center. However, ascribing a given solvent water molecule as being “hydrogen bonded” to the solute species only by analysis of the pair-wise atom–atom RDFs is equivalent to imposing only a single criterion for definition of a hydrogen bond—the distance criterion.

This means that if the N5... $O_w$  distance is smaller than a threshold value (e.g., the minimum between the first- and second-shell RDF peaks, which is 3.05 Å in this case) the solvent and solute species will be considered to be hydrogen bonded. However, this is obviously not always the case. Due to the thermal motions in the liquid, although certain solvent molecules may approach closely the solute species, their orientation may not be favorable from either energetic or orientational, that is, geometric aspect (characteristic of the hydrogen bond interaction). It is, therefore, necessary to impose two additional criteria to define precisely the hydrogen bond within a liquid (thermally fluctuating medium). The necessity for imposing the energetic criterion can be clearly seen from Figure 3 where the solute–solvent pair-wise interaction energies are plotted against the distances between the centers of masses of the solute and solvent molecules.

Obviously, even for very small  $R_{cm-cm}$  values, the pair-wise intermolecular interaction energies may be zero or positive. To select the energy cut-off criterion, we constructed the histogram of solute–solvent pair-wise interaction energies as computed from the MC potential (Fig. 4).

The singularity at  $E = 0$  is due to the large number of weak ion-dipolar pair interactions at large solute–solvent distances, with the solvent molecules which are, at these distances, irregularly distributed due to thermal motions within the liquid. However, the additional, albeit much smaller peak at lower-energy values (with a maximum appearing somewhat below  $-4$  kcal mol $^{-1}$  in the case of both compounds), corresponds to a particular population of more strongly interacting solvent molecules with the solute. To cut-off what is out of this particular population, we impose an energy criterion of  $-2.0$  kcal mol $^{-1}$  (the value that roughly corresponds to the minimum between the two bell-shaped curves in the histogram on Fig. 4a; the corresponding energy value which could be deduced from the histogram on Fig. 4b) was  $-3.0$  kcal mol $^{-1}$ ). Of all first-shell water molecules which satisfy both the distance and energetic criterion for H-bond definition, we also considered their actual orientation with respect to the solute species, which also has to be an appropriate one in the case of H-bonding arrangement. To define this orientation quantitatively, we consider the distribution of the  $N5O_wH_w$  angles for all of the first-shell waters satisfying the previous two criteria. The



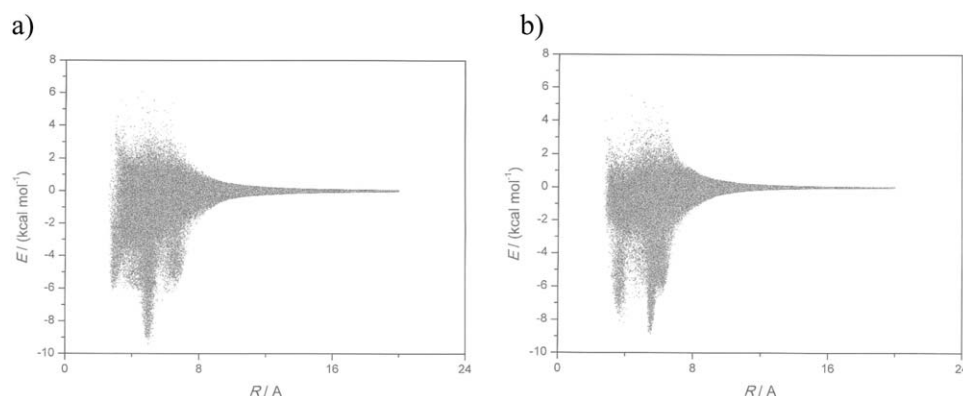


**Figure 3.** Distribution of pair interaction energies as a function of intermolecular distance  $R$  (between molecular centers-of-mass): a) 5-azauracil and b) 6-azauracil.

corresponding first-shell selected angular distribution function is given in Figure 5.

As obvious from Figure 5a, the pronounced peak at very low angles corresponds to favorable H-bonding arrangements of the first-shell water molecules around this particular center (N5) of the solute species, acting as H-bonding proton acceptor. The minimum between the two most pronounced peaks in the considered angular distribution function is, therefore, a natural angular criterion for the H-bond existence ( $60^\circ$  in this studied case). Imposing these three criteria, leads to a total number of 0.34 hydrogen bonds in which, on average, the N5 center participates as a proton acceptor. As will become clear later, such a small number of proton-donating solvent OH groups around the N5 center are due to the competitive H-bond proton-accepting center O8. Repeating the same procedure for other H-bonding accepting (O7 and O8) and H-bond donating centers (N1H10 and N3H11) within tautomer **A** of 5-azauracil led to the results for the average number of H-bonds in which each particular center, which are summarized in Table 1. Note that the much less pronounced peak in Figure 5b, corresponds to the notably smaller average number of H-bonds accepted by the N4 center in 6-AU (see Table 1 and the discussion below).

If one takes a closer look at the relative values of the average numbers of donated or accepted H-bonds of the tautomeric form **A** of 5-AU in aqueous media, it appears that the trends may be straightforwardly understood. For example, as mentioned before, the relatively small number of H-bonds

formed with the solvent molecules in which (on average) the N5 center acts as a proton acceptor may be attributed to the proximity of the O8 center, which is more exposed and also a better H-bond proton acceptor. Conversely, the larger number of H-bonds in which (on average) the O8 center acts as a proton acceptor in comparison to the O7, one can be attributed to the more-exposed character of the O8 center in the tautomer **A**. At the same time, the N3H11 bond of 5-azauracil appears to be a more efficient H-bond proton donor than the N1H10 one, due to the presence of only one proximal oxygen atom (the O7 center) in this case (as compared to two—O7 and O8 in the case of N1H10). Therefore, exploring the section of the PES of the 5-AU tautomer **A** with four-water molecules hydrogen bonded to the O7, O8, H10, and H11 centers as a starting point for the water-assisted tautomerization by micro-hydration approach appears to be justified by the hydration behavior of this form in diluted aqueous solutions. This could, therefore, be a good model representing the real situation in the vicinity of tautomer **A** in bulk water in the course of tautomerization process.

Similar analyses were carried out for tautomers **B** and **D** of 5-AU. Detailed results, including all of the relevant RDF plots, as well as plots with relevant angular distributions are available from the authors on request. The numbers of accepted and donated H-bonds (on average) from each intramolecular site of structures **B** and **D** are given in Table 1.

Concerning structure **B** and **D**, the same logic of populating the explicit nearest-neighbour solvent water molecules around

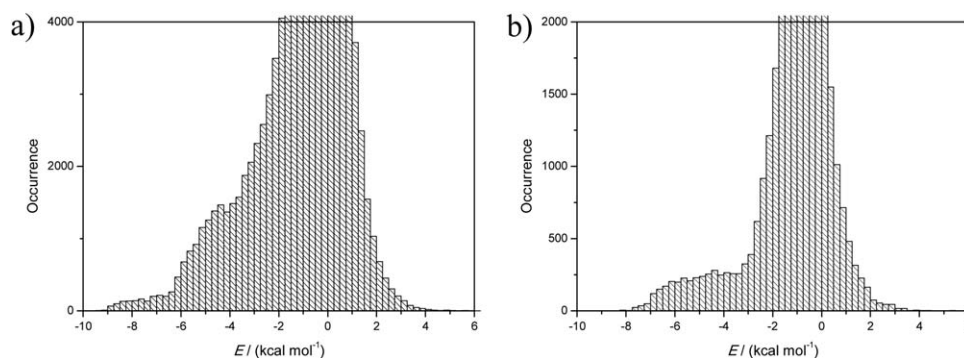


**Figure 4.** Histogram of distribution of pair interaction energies computed from the equilibrated MC run: a) 5-azauracil and b) 6-azauracil.

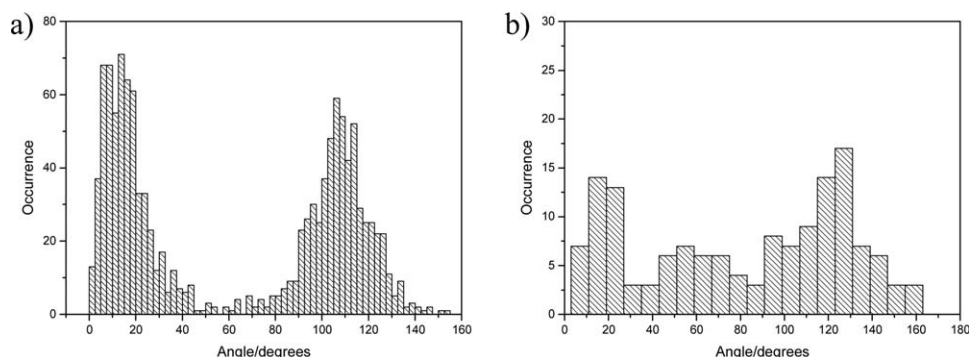


**Figure 5.** Histogram of distribution of the  $N5O_wH_w$  angles for all the first-shell waters around 5-azauracil a) and  $N4O_wH_w$  angles for all the first-shell waters around 6-azauracil b) computed from the equilibrated MC run.

5-azauracil as in the case of structure **A** was implemented. The number of explicit waters was kept at the smallest possible value ensuring reliable results at acceptable computational cost. Care was also taken to ensure inclusion of additional water molecule at the sites at which solvent molecule clustering is possible.

Analogs analyses as those carried out for 5-AU have also been performed for all minima on the 6-AU ground-state PES (**A**, **B**, **C**, and **D** in Fig. 1). Table 1 compiles the most important numerical data concerning the average number of donated and accepted hydrogen bonds on interaction with the solvent molecules. Detailed results and plots are available from the authors on request. The evident differences in local hydration

behavior in the case of 5- and 6-AU may be ascribed to the differences in the solute–solvent noncovalent intermolecular interactions due to charge redistribution on change of the position of the additional nitrogen atom in uracil, as well as to the accompanying steric effects.

#### Tautomeric equilibrium of 5-azauracil and 6-azauracil

Here, we consider the solvent effect on the tautomeric conversion of 5-azauracil and 6-azauracil through a microhydration model. In this model, the two pairs of water molecules forming a cluster are situated between the two pairs of N–H and C = O groups. The values of the free energies ( $\Delta G_{298}$ ) for four-hydrated complexes of dioxo and hydroxy tautomers of **5-AU**

**Table 1.** The average number of H-bonds with the solvent water molecules in which each particular center within 5-azauracil and 6-azauracil participates (either as proton donor or as proton acceptor), computed by the procedure described in the text.

Center	Average No. of accepted H-bonds	Average No. of donated H-bonds	Center	Average No. of accepted H-bonds	Average No. of donated H-bonds
5-azauracil			6-azauracil		
Tautomer A			Tautomer A		
N5	0.34	–	N4	0.10	–
O7	1.13	–	O7	1.15	–
O8	1.26	–	O8	0.98	–
N1H10	–	0.60	N1H10	–	0.84
N3H11	–	0.74	N3H11	–	0.62
Tautomer B			Tautomer B		
N3	0.69	–	N3	1.15	–
N5	0.85	–	N4	1.02	–
O7	0.04	–	O7	0.17	–
O8	1.28	–	O8	2.04	–
N1H10	–	0.88	N1H10	–	0.88
O7H11	–	0.94	O7H11	–	0.17
Tautomer D			Tautomer D		
N1	1.40	–	N1	0.50	–
N5	0.67	–	N4	0.06	–
O7	1.64	–	O7	1.40	–
O8	0.32	–	O8	0.10	–
N3H11	–	0.83	N3H11	–	0.56
O8H10	–	0.83	O8H10	–	0.97
			Tautomer C		
			N1	0.65	–
			N4	0.02	–
			O7	0.04	–
			O8	1.60	–
			N3H11	–	0.82
			O7H10	–	0.90

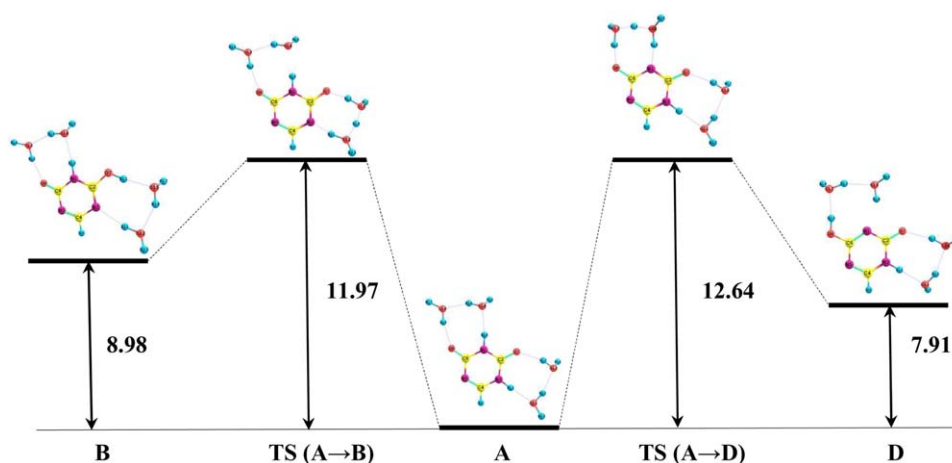


**Figure 6.** C-PCM/MP2/6-31 + G(d, p) calculated relative energies ( $\Delta G_{298}$ ) and energy barriers ( $\Delta G_{298}^{\ddagger}$ ) ( $\text{kcal mol}^{-1}$ ) for the tautomeric conversions in 5-azauracil.

(Fig. 6) and **6-AU** (Fig. 7) obtained at MP2/6-31 + G(d, p), C-PCM/MP2/6-31 + G(d, p) and CCSD(T)//MP2/6-31 + G(d, p) levels are given in Table 2.

**5-azauracil.** According to our calculations the most stable is the complex of the 2,4-dioxo form **A** of **5-AU** followed by the hydrated hydroxy forms **D** and **B** at all theoretical levels. The MP2 calculated relative free energy difference between the four-hydrated complexes of **A** and **D** ( $7.59 \text{ kcal mol}^{-1}$ ) is smaller than that between the **A** and **B** ones ( $9.57 \text{ kcal mol}^{-1}$ ). Taking into account the electron correlation of higher order at CCSD(T) level, a slight decrease of the energy differences between **A** +  $4\text{H}_2\text{O}$  and **B** +  $4\text{H}_2\text{O}$  by  $0.26 \text{ kcal mol}^{-1}$  and **A** +  $4\text{H}_2\text{O}$  and **D** +  $4\text{H}_2\text{O}$  by  $0.32 \text{ kcal mol}^{-1}$  is observed. The opposite tendency exists when we consider a model in which the structure of the four-hydrated tautomer is optimized taking into account the solvent as a continual polarizable medium as compared to the bare cluster in the gas phase. A slight increase of the differences by  $0.27 \text{ kcal mol}^{-1}$  for **B** +  $4\text{H}_2\text{O}$  and  $0.92 \text{ kcal mol}^{-1}$  for **D** +  $4\text{H}_2\text{O}$  is observed at C-PCM level. Due to these differences (Table 1) the populations

of species **D** and **B** are  $1.6 \times 10^{-4}\%$  and  $6.1 \times 10^{-6}\%$ , respectively. Species **C** and **E** are more than  $10 \text{ kcal mol}^{-1}$  less stable than tautomer **A** at all computational levels and are not further considered in our analysis.

In the case of four-hydrated complex of **5-AU**, the proton transfer activation energies for the two parallel reactions **A** → **B** and **A** → **D** are very close (Fig. 6). The reaction barrier of **A** → **B** calculated at MP2/6-31 + G(d, p) level of theory amounts to  $16.50 \text{ kcal mol}^{-1}$ , which is lower by only  $0.16 \text{ kcal mol}^{-1}$  than that of the **A** → **D** proton transfer reaction. When the electron correlation of higher order is taken into account (at CCSD(T) level), the height of the free energy barrier for the two tautomeric conversions is larger by  $2 \text{ kcal mol}^{-1}$ . The exactly reversed situation is observed when the solvent effect by C-PCM method is considered: the barriers decrease by  $4.53 \text{ kcal mol}^{-1}$  for the **A** → **B** reaction and by  $4.02 \text{ kcal mol}^{-1}$  for the **A** → **D** reaction. Both investigated proton transfer reactions involve concerted atomic movement.

TS theory was applied to estimate the rate constants  $k$  of the reactions **A** → **B** and **A** → **D** using the Eyring equation. The computed rate constants  $k$  of the proton transfer

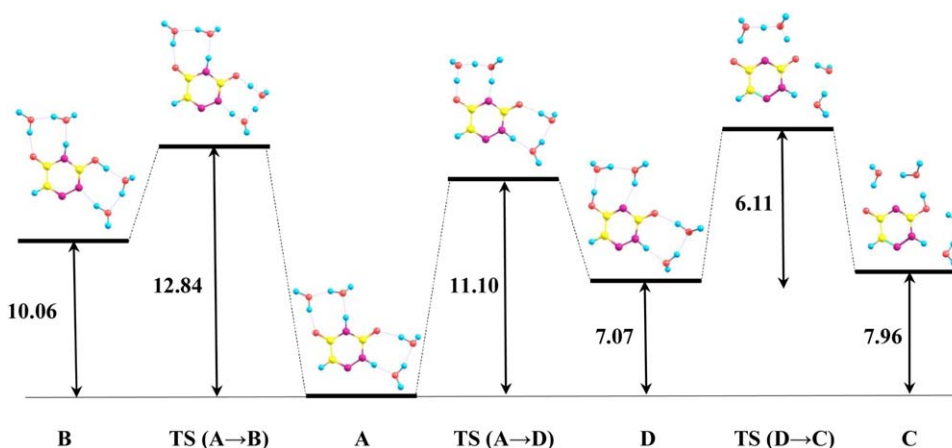


**Figure 7.** C-PCM/MP2/6-31 + G(d, p) calculated relative energies ( $\Delta G_{298}$ ) and energy barriers ( $\Delta G_{298}^{\ddagger}$ ;  $\text{kcal mol}^{-1}$ ) for the tautomeric conversions in 6-azauracil.



**Table 2.** Relative free energies,  $\Delta G_{298}$  (kcal mol<sup>-1</sup>), of the tautomers of **5-AU** and **6-AU** (Fig. 1) calculated at different computational levels.

Species	CCSD(T)/ 6-31 + G(d, p)// MP2/6-31 + G(d, p)	MP2/6-31 + G(d, p)	C-PCM/MP2/6- 31 + G(d, p)	Population (%)
	$\Delta G_{298}$	$\Delta G_{298}$	$\Delta G_{298}$	
<b>5-AU</b>				
<b>A</b> + 4H <sub>2</sub> O	0.00	0.00	0.00	99.999
<b>B</b> + 4H <sub>2</sub> O	9.31	9.57	9.84	$6.1 \times 10^{-6}$
<b>C</b> + 4H <sub>2</sub> O	15.49	15.54	12.29	$9.8 \times 10^{-8}$
<b>D</b> + 4H <sub>2</sub> O	7.27	7.59	7.91	$1.6 \times 10^{-4}$
<b>E</b> + 4H <sub>2</sub> O	10.78	11.26	11.29	$5.3 \times 10^{-7}$
<b>6-AU</b>				
<b>A</b> + 4H <sub>2</sub> O	0.00	0.00	0.00	99.999
<b>B</b> + 4H <sub>2</sub> O	11.74	11.65	10.06	$4.2 \times 10^{-6}$
<b>C</b> + 4H <sub>2</sub> O	12.26	12.01	7.96	$1.5 \times 10^{-4}$
<b>D</b> + 4H <sub>2</sub> O	7.13	6.84	7.07	$6.6 \times 10^{-4}$
<b>E</b> + 4H <sub>2</sub> O	13.78	13.07	10.77	$1.3 \times 10^{-6}$

in **5-AU** are listed in Table 3. On the basis of the computed free energy barriers of the two tautomeric reactions, the rate constants are largest at C-PCM/MP2/6-31 + G(d, p) level of theory ( $k = 10^3$ – $10^4$  s<sup>-1</sup>). Although the constants computed at MP2 (ca. 4–5 s<sup>-1</sup>) and CCSD(T) ( $10^{-1}$ s<sup>-1</sup>) levels are smaller, both of these parallel tautomeric conversions should occur. The **A** → **B** reaction is certainly kinetically preferred while thermodynamic arguments give preference to the reaction **A** → **D**.

**Table 3.** Calculated energy barriers,  $\Delta G_{298}$  (in kcal mol<sup>-1</sup>), for **A** → **B**, **A** → **D**, and **D** → **C** reactions in four-hydrated complexes of **5-AU** and **6-AU**.

Computational level	$\Delta G_{298}$	$k$	$\nu^\#$
<b>5-azauracil</b>			
<b>A</b> + 4H <sub>2</sub> O → <b>B</b> + 4H <sub>2</sub> O			
C-PCM/MP2/6-31 + G(d, p)	11.97	$1.04 \times 10^4$	460.34 <i>i</i>
MP2/6-31 + G(d, p)	16.50	4.98	978.78 <i>i</i>
CCSD(T)/6-31 + G(d, p)/ /MP2/6-31 + G(d, p)	18.50	$1.70 \times 10^{-1}$	
<b>A</b> + 4H <sub>2</sub> O → <b>D</b> + 4H <sub>2</sub> O			
C-PCM/MP2/6-31 + G(d, p)	12.64	$3.37 \times 10^3$	818.26 <i>i</i>
MP2/6-31 + G(d, p)	16.66	3.80	994.91 <i>i</i>
CCSD(T)/6-31 + G(d, p)/ /MP2/6-31 + G(d, p)	18.68	$1.26 \times 10^{-1}$	
<b>6-azauracil</b>			
<b>A</b> + 4H <sub>2</sub> O → <b>B</b> + 4H <sub>2</sub> O			
C-PCM/MP2/6-31 + G(d, p)	12.84	$2.40 \times 10^3$	726.9 <i>i</i>
MP2/6-31 + G(d, p)	18.05	$3.60 \times 10^{-1}$	1031.1 <i>i</i>
CCSD(T)/6-31 + G(d, p)/ /MP2/6-31 + G(d, p)	20.35	$7.50 \times 10^{-3}$	
<b>A</b> + 4H <sub>2</sub> O → <b>D</b> + 4H <sub>2</sub> O			
C-PCM/MP2/6-31 + G(d, p)	11.10	$4.53 \times 10^4$	748.8 <i>i</i>
MP2/6-31 + G(d, p)	15.73	$1.83 \times 10^1$	937.8 <i>i</i>
CCSD(T)/6-31 + G(d, p)/ /MP2/6-31 + G(d, p)	18.00	$3.96 \times 10^{-1}$	
<b>D</b> + 4H <sub>2</sub> O → <b>C</b> + 4H <sub>2</sub> O			
C-PCM/MP2/6-31 + G(d, p)	6.11	$2.06 \times 10^8$	553.2 <i>i</i>
MP2/6-31 + G(d, p)	14.57	$1.29 \times 10^2$	565.6 <i>i</i>
CCSD(T)/6-31 + G(d, p)/ /MP2/6-31 + G(d, p)	16.29	7.10	

The calculated values of barriers for the forward reactions are given. Rate constants are in s<sup>-1</sup>. Imaginary frequencies  $\nu^\#$  are in cm<sup>-1</sup>.

**6-azauracil.** According to results presented in Table 2, the complex of the 2,4-dioxo form **A** of **6-AU** is the most stable followed by the hydrated hydroxy form **D** at all theoretical levels. The MP2 and CCSD(T) calculated relative free energy difference between all four-hydrated complexes are very similar. The hydrated forms of tautomers **B**, **C**, and **E** are close in energy. When we consider a model in which the structure of the four-hydrated tautomer is optimized taking into account the solvent as medium compared to the cluster in the gas phase, two-hydrated tautomer couples have close relative energies—**C** and **D** and **B** and **E** (Table 2). Decrease of the energy differences for **B** + 4H<sub>2</sub>O, **C** + 4H<sub>2</sub>O, and **E** + 4H<sub>2</sub>O is observed at C-PCM level compared to MP2 and CCSD(T) levels. The exception is **D** + 4H<sub>2</sub>O where there is no substantial change. Due to these differences (Table 2), the populations of the hydrated tautomers **D** and **C** are  $6.6 \times 10^{-4}\%$  and  $1.5 \times 10^{-4}\%$ , respectively.

The solvent-assisted proton transfer activation energies for the two parallel reactions **A** → **B** and **A** → **D** of **6-AU** (Fig. 7) are close, but the situation is different from that for **5-AU**. The reaction barrier of **A** → **B** calculated at C-PCM/MP2/6-31 + G(d, p) level of theory amounts to 12.84 kcal mol<sup>-1</sup>, which is higher by 1.74 kcal mol<sup>-1</sup> compared to that of the **A** → **D** reaction. The computed rate constants  $k$  of the proton transfer in **6-AU** are listed in Table 3. The **A** → **D** reaction is kinetically and thermodynamically preferred as compared to the **A** → **B** one. The rate constant  $k$  of the **A** → **D** reaction is  $4.53 \times 10^4$  s<sup>-1</sup> and it is an order of magnitude higher than that of the **A** → **B** one (see Table 3). At the same time, tautomer **D** is by 2.99 kcal mol<sup>-1</sup> more stable than tautomer **B**. As the activation barrier of the reaction **D** → **C** is only 6.11 kcal mol<sup>-1</sup> (Fig. 7) and the respective rate constant  $k$  is  $2.06 \times 10^8$  s<sup>-1</sup>, it seems more probably that the two contiguous reactions, **A** → **D** and **D** → **C**, could occur in water solution.

## Conclusions

This study devoted to water-assisted proton transfer in 5-azauracil and 6-azauracil reveals different pictures for these two compounds. According to C-PCM/MP2/6-31 + G(d, p) calculations, the most stable is the four-hydrated complex of the dioxo form **A** (99.99%) followed by the hydrated hydroxy forms **D** ( $1.6 \times 10^{-4}\%$ ) and **B** ( $6.1 \times 10^{-6}\%$ ) of 5-azauracil. The calculated proton transfer activation energies for the parallel reactions **A** → **B** and **A** → **D** are close—11.97 kcal mol<sup>-1</sup> for the first reaction and 12.64 kcal mol<sup>-1</sup> for the second one. Both investigated proton transfer reactions involve concerted atomic movement. The computed rate constants are in the range of  $10^3$ – $10^4$  s<sup>-1</sup>. The **A** → **B** reaction is a kinetically feasible process while the **A** → **D** reaction is thermodynamically preferred.

**6-azauracil** should exist in three forms: mainly dioxo form **A** (99.99%) and two close in energy hydroxy tautomers—**D** ( $6.6 \times 10^{-4}\%$ ) and **C** ( $1.5 \times 10^{-4}\%$ ). As the activation barriers of the tautomeric reactions **A** → **D** and **D** → **C** are calculated to be 11.10 kcal mol<sup>-1</sup> ( $k = 4.53 \times 10^4$  s<sup>-1</sup>) and 6.11 kcal mol<sup>-1</sup> ( $k = 2.06 \times 10^8$  s<sup>-1</sup>), respectively, it seems probable that the

two contiguous reactions,  $A \rightarrow D$  and  $D \rightarrow C$ , should occur in water solution and the hydroxyl tautomers **D** and **C** should be coexisting with tautomer **A**.

**Keywords:** 5-azauracil • 6-azauracil • proton transfer • tautomerism • *ab initio*

How to cite this article: N. Markova, L. Pejov, V. Enchev *Int. J. Quantum Chem.* **2015**, *115*, 477–485. DOI: 10.1002/qua.24871

- [1] I. C. Martin, *J. Comput. Aided Mol. Des.* **2009**, *23*, 693.
- [2] J. Elguero, Tautomerism in Brenner's Encyclopedia of Genetics, 2nd ed., Vol. 7; Elsevier Inc., **2013**, pp. 18–22.
- [3] P. O. Löwdin, *Rev. Mod. Phys.* **1963**, *35*, 724.
- [4] P. O. Löwdin, *Adv. Quantum Chem.* **1966**, *2*, 213.
- [5] I. Alkorta, P. Goya, J. Elguero, S. P. Singh, *Natl. Acad. Sci. Lett.* **2007**, *30*, 139.
- [6] A. R. Katritzky, C. D. Hall, B. E.-D. M. El-Gendy, B. Draghici, *J. Comput. Aided Mol. Des.* **2010**, *24*, 475.
- [7] Y. Cha, C. J. Murray, J. P. Klinman, *Science* **1989**, *243*, 1325.
- [8] Y.-I. Lin, J. Gao, *Biochemistry* **2010**, *49*, 84.
- [9] L. Gorb, J. Leszczynski, *J. Am. Chem. Soc.* **1998**, *120*, 5024.
- [10] J. Gu, J. Leszczynski, *J. Phys. Chem. A* **1999**, *103*, 2744.
- [11] N. N. Zhanpeisov, W. W. Cox, J. Leszczynski, *J. Phys. Chem. A* **1999**, *103*, 4564.
- [12] M. K. Shukla, J. Leszczynski, *J. Mol. Struct. Theochem* **2000**, *529*, 99.
- [13] M. K. Shukla, J. Leszczynski, *J. Phys. Chem. A* **2000**, *104*, 3021.
- [14] Z. Smedarchina, W. Siebrand, A. Fernandez-Ramos, L. Gorb, J. Leszczynski, *J. Chem. Phys.* **2000**, *112*, 566.
- [15] Y. Podolyan, L. Gorb, J. Leszczynski, *Int. J. Mol. Sci.* **2003**, *4*, 410.
- [16] M. Hanus, F. Ryjacek, M. Kabelac, T. Kubar, T. V. Bogdan, S. A. Trygubenko, P. Hobza, *J. Am. Chem. Soc.* **2003**, *125*, 7678.
- [17] D. Ahn, S. Lee, B. Kim, *Chem. Phys. Lett.* **2004**, *390*, 384.
- [18] Y. Podolyan, L. Gorb, J. Leszczynski, *J. Phys. Chem. A* **2005**, *109*, 10445.
- [19] N. Markova, V. Enchev, I. Timcheva, *J. Phys. Chem. A* **2005**, *109*, 1981.
- [20] N. Markova, V. Enchev, G. Ivanova, *J. Phys. Chem. A* **2010**, *114*, 13154.
- [21] A. Furmanchuk, O. Isayev, L. Gorb, O. V. Shishkin, D. M. Hovorun, J. Leszczynski, *Phys. Chem. Chem. Phys.* **2011**, *13*, 4311.
- [22] S. Morprugo, M. Bossa, G. O. Morprugo, *Adv. Quantum Chem.* **2000**, *36*, 169.
- [23] V. Enchev, N. Markova, S. Angelova, *Chem. Phys. Res. J.* **2007**, *1*, 1.
- [24] F. J. Lakner, H. Xia, A. Pervin, J. R. Hammaker, K. G. Jahangiri, M. K. Dalton, A. Khvat, A. Kiselyov, A. V. Ivachtchenko, *Tetrahedron Lett.* **2005**, *46*, 5325.
- [25] J. Jonas, M. Horak, A. Piskala, J. Gut, *Collect. Czech. Chem. Commun.* **1962**, *27*, 2754.
- [26] R. K. Pike, *Org. Magn. Reson.* **1976**, *8*, 224.
- [27] B. S. Potter, R. A. Palmer, R. Withnall, B. Z. Chowdhry, *New J. Chem.* **1999**, *1*, 117.
- [28] D. Ajò, M. Casarin, G. Granozzi, I. Fragalà, *Chem. Phys. Lett.* **1981**, *80*, 188.
- [29] P. Singh, D. J. Hodgson, *J. Chem. Soc. Chem. Commun.* **1973**, *13*, 439.
- [30] W. Seibert, *Chem. Ber.* **1947**, *80*, 494.
- [31] E. A. Falco, E. Pappas, G. H. Hitchings, *J. Am. Chem. Soc.* **1956**, *78*, 1938.
- [32] C. J. Grundmann, H. Schroeder, R. F. W. Rätz, *J. Org. Chem.* **1958**, *23*, 1522.
- [33] C. Cristescu, J. Marcus, *Pharmazie* **1961**, *16*, 135.
- [34] C. A. Lovelette, *J. Heterocycl. Chem.* **1979**, *16*, 1649.
- [35] W. S. Sheldrick, D. Neumann, *Inorganica Chim. Acta* **1994**, *223*, 131.
- [36] N. A. Al-Awadi, Y. A. Ibrahim, H. H. Dib, M. R. Ibrahim, B. J. George, M. R. Abdallah, *Tetrahedron* **2006**, *62*, 6214.
- [37] M. Habibi-Khorassani, M. T. Maghsoodlou, A. Ebrahimi, M. A. Kazemian, M. Zakarianejad, *Phosphorus Sulfur Silicon Relat. Elem.* **2009**, *184*, 2959.
- [38] C. Lifshitz, E. D. Bergmann, B. Pullman, *Tetrahedron Lett.* **1967**, *46*, 4583.
- [39] P. Singh, D. J. Hodgson, *Acta Crystallogr. B* **1974**, *30*, 1430.
- [40] R. Zahradnik, J. Koutecky, J. Jonas, *J. Gut Collect. Czech. Chem. Commun.* **1963**, *28*, 1499.
- [41] J. Fulara, M. J. Nowak, L. Lapinski, A. Les, L. Adamowicz, *Spectrochim. Acta A* **1991**, *47*, 595.
- [42] A. Les, I. Ortega-Blake, *Int. J. Quantum Chem.* **1986**, *30*, 225.
- [43] H. H. Corzo, O. Dolgounitcheva, V. G. Zakrzewski, J. V. Ortiz, *J. Phys. Chem. A* **2014**, *118*, 6908.
- [44] J. Chen, A. Buonaugurio, O. Dolgounitcheva, V. G. Zakrzewski, K. H. Bowen, J. V. Ortiz, *J. Phys. Chem. A* **2013**, *117*, 1079.
- [45] K. Wittine, M. Stipković Babić, M. Košutić, M. Cetina, K. Rissanen, S. Kraljević Pavelić, A. Tomljenović Paravić, M. Sedić, K. Pavelić, M. Mintas, *Eur. J. Med. Chem.* **2011**, *46*, 2770.
- [46] M. Cossi, N. Rega, G. Scalmani, V. Barone, *J. Comput. Chem.* **2003**, *24*, 669.
- [47] S. Miertus, E. Scrocco, J. Tomasi, *Chem. Phys.* **1981**, *55*, 117.
- [48] J. Tomasi, M. Persico, *Chem. Rev.* **1994**, *94*, 2027.
- [49] C. J. Cramer, D. G. Truhlar, *Chem. Rev.* **1999**, *99*, 2161.
- [50] M. Orozco, F. J. Luque, *Chem. Rev.* **2000**, *100*, 4187.
- [51] J. Tomasi, B. Mennucci, R. Cammi, *Chem. Rev.* **2005**, *105*, 2999.
- [52] C. J. Cramer, D. G. Truhlar, *Acc. Chem. Res.* **2008**, *41*, 760.
- [53] A. V. Marenich, C. J. Cramer, D. G. Truhlar, *J. Phys. Chem. B* **2009**, *113*, 6378.
- [54] I. Soteras, C. Curutchet, A. Bidon-Chanel, M. Orozco, F. J. Luque, *J. Mol. Struct. Theochem* **2005**, *727*, 29.
- [55] A. Klamt, G. Schüürmann, *J. Chem. Soc. Perkin Trans. 2* **1993**, 799.
- [56] A. Klamt, *J. Phys. Chem.* **1995**, *99*, 2224.
- [57] A. Klamt, V. Jonas, T. Bürger, J. C. W. Lohrenz, *J. Phys. Chem. A* **1998**, *102*, 5074.
- [58] V. Barone, M. Cossi, *J. Phys. Chem.* **1998**, *102*, 1995.
- [59] S. Canuto, K. Coutinho, In DICE: A Monte Carlo Program for Molecular Liquid Simulation; University of São Paulo: Brazil, **1997**.
- [60] H. J. C. Berendsen, J. P. M. Postma, W. F. van Gunsteren, J. Hermans, *Intermolecular Forces*; Reidel: Dordrecht, Germany, **1981**; p. 331.
- [61] C. M. Breneman, K. B. Wiberg, *J. Comput. Chem.* **1990**, *11*, 361.
- [62] W. L. Jorgensen, D. S. Maxwell, J. Tirado-Rives, *J. Am. Chem. Soc.* **1996**, *118*, 11225.
- [63] C. Gonzales, H. B. Schlegel, *J. Chem. Phys.* **1989**, *90*, 2154.
- [64] G. D. Purvis, III, R. J. Bartlett, *J. Chem. Phys.* **1982**, *76*, 1910.
- [65] K. Raghavachari, G. W. Trucks, J. A. Pople, M. Head-Gordon, *Chem. Phys. Lett.* **1989**, *157*, 479.
- [66] P. Piecuch, S. A. Kucharski, K. Kowalski, M. Musail, *Comput. Phys. Commun.* **2002**, *149*, 71.
- [67] J. L. Bentz, R. M. Olson, M. S. Gordon, M. W. Schmidt, R. Kendall, *Comput. Phys. Commun.* **2007**, *176*, 589.
- [68] R. M. Olson, J. L. Bentz, R. A. Kendall, M. W. Schmidt, M. S. Gordon, *J. Comput. Theor. Chem.* **2007**, *3*, 1312.
- [69] (a) M. W. Schmidt, K. K. Baldrige, J. A. Boatz, S. T. Elbert, M. S. Gordon, J. H. Jensen, S. Koseki, N. Matsunaga, K. A. Nguyen, S. Su, T. L. Windus, M. Dupuis, J. A. Montgomery, *J. Comput. Chem.* **1993**, *14*, 1347; (b) M. S. Gordon and M. W. Schmidt, *In Theory and Applications of Computational Chemistry: The First Forty Years*, C. E. Dykstra, G. Frenking, K. S. Kim, G. E. Scuseria, Eds.; Elsevier: Amsterdam, **2005**; pp. 1167.

Received: 10 November 2014  
Revised: 7 January 2015  
Accepted: 9 January 2015  
Published online 29 January 2015